arXiv:hep-ph/0506318v1 30 Jun 2005

# Two loop renormalization of the magnetic coupling and non-perturbative sector in hot QCD

P. Giovannangeli
*Department of Theoretical Physics, University of Bielefeld, Germany*
*E-mail: giovanna@physik.uni-bielefeld.de*

**Abstract**

The goal of this paper is two-fold. The first aim is to present a detailed version of the computation of the two-loop renormalization of the magnetic coupling in hot QCD. The second is to compare with lattice simulations the string tension of a spatial Wilson loop using the result of our two-loop computation.

## 1 Introduction

Several breakthroughs have been made in the last few years in the computation of high order terms of observables in QCD at high temperature. In particular the pressure has been determined perturbatively up its last perturbative term namely $g^6 ln(g)$, where $g(T)$ is the QCD running coupling [1]. More than numerical results, these computations have given some insights for the knowledge of the convergence of perturbation theory in hot QCD.

Indeed, due to infrared divergences, perturbation theory in hot QCD is limited [2]. At a given order in the weak coupling expansion, an infinite set of Feynman graphs will contribute to the thermal mean of an observable. This order depends on the observable or thermodynamic quantity that is computed. For example, the pressure of the gluon gas can be computed perturbatively up to but not including the order $g^6$ whereas problems arise at next-to-leading order for the electric Debye mass. So, despite asymptotic freedom, a non-perturbative part still remains in the hot QCD phase.

Facing such a problem when one does perturbation theory and wanting to apply it in realistic cases renders mandatory the need for a coherent way to treat the perturbative expansion, taking care of infrared divergences. Whatever the approach used to get rid of infrared divergences, it is based on the dynamical screening of gluon field in the plasma, namely the Debye effect that gives a natural infrared regulator.

We are going to work in the framework of Dimensional Reduction (D.R.) [3,4]. It is based on the systematic construction of effective theories for each physical scales in the QCD plasma, namely for external momenta of order $T$, $gT$ and $g^2T$ . This approch combined with $3D$ simulations has provided insights in phase transition in the Standard Model [5] and also allows to compute the perturbative terms of the QCD pressure [1].

At really high temperature and large scales, within this method, the QCD plasma is described by a magnetostatic Lagrangian whose leading term is a three-dimensional (3D) Yang-Mills whose coupling is computed via perturbation theory. The important point is that the magnetostatic Lagrangian that describes hot QCD for external momenta of order $g^2T$, contains all the non-perturbative physics in the region where the coupling is small.

Our purpose is first to compute the effective coupling of this 3D Yang-Mills [6] by integrating out the electrostatic Debye scale of order $gT$ and then to use this result in order to investigate, thanks to lattice simulations, how our actual knowledge of the magnetostatic part is sufficient to encompass the whole non-perturbative high T physics in the case of the spatial Wilson loop. This article is composed as follows:
Section (2) is a brief recall of the principles of D.R.. Section (3) focuses on the magnetostatic action. Section (4) shows the steps to perform the two-loop computation. Section (5)

is the body of the computation with all intermediate and final result. Finally the last section will deal with the applications of magnetostatic physics in the QCD plasma, looking at an observable, the so-called Wilson Loop.

## 2 Dimensional reduction perturbation theory

Due to infrared divergences, perturbation theory in hot QCD is limited. That means that the analytical computation of the thermal mean of an observable is confronted with two main problems. The first one is to make a coherent perturbation theory until it breaks down. The second one is to evaluate numerically and with the most precision the contribution of the non perturbative sector. Indeed whatever the observable you will consider, the weak coupling expansion will be limited.

For a review of effective theories and dimensional reduction see [7]. At equilibrium, a thermodynamic system is described by its partition function:

$$Z(\beta) = Tr_{phys} \exp(-\beta H) \tag{1}$$

where $H$ is the Hamiltonian of the system. In the imaginary time formalism, the latter can be written as a path integral:

$$Z(\beta) = \int D\phi D\psi \exp(-\int_0^{\frac{1}{T}} \int d^3x dt \mathcal{L}_{\mathcal{E}}) \tag{2}$$

with $\phi$ a bosonic field and $\psi$ a fermionic field, with the boundary conditions $\phi(x, \frac{1}{T}) = \phi(x, 0)$ and $\psi(x, \frac{1}{T}) = -\psi(x, 0)$. So, technically, one is dealing with quantum field theory on a cylinder with a compact time direction, as in Kaluza-Klein theories. The periodicity of the time dimension is $\frac{1}{T}$. So, for large $T$, i.e. larger than the typical momentum scale that one considers, one expects to have an effective three dimensional theory. Due to time periodicity, as for massless bosonic fields, the euclidean propagator reads:

$$\frac{1}{p^2} = \frac{1}{\vec{p}^2 + (2\pi n T)^2}. \tag{3}$$

The massless bosons have a mass $2\pi n T$ that is going to regularize the infrared. But for $n = 0$, i.e static modes, infrared problems will still be there. Let us be more precise.

In the case of QCD, we have:

$$\mathcal{L}_{QCD} = \frac{1}{2} Tr F_{\mu\nu} F_{\mu\nu} + \sum_{i=1}^{N_f} \bar{\psi}_i (\gamma_\mu D_\mu + m_i) \psi_i. \tag{4}$$

As quarks have no zero Matsubara frequency, they always appear as heavy modes.

But what is going to happen for the $A_\mu$ static modes? Part of the problem will be solved because for electric static mode $A_0$, there is Debye screening that is going to regularize the infrared. Indeed, like in classical plasmas, the chromoelectric field is screened in such a state of matter. The electrostatic potential will behave as Yukawa potential, and large distance contribution will be suppressed thanks to the exponential fall-off of such a potential. We describe below in a more quantitative way what is going to happen.

In fact there will be different physical scales in the plasma, to which different effective theories will correspond. Let $p$ be the value of the external momentum in the plasma.

- for $p \sim T$, the theory is QCD for hard modes ( with $n$ nonzero)
- for $p \sim gT$, we have integrated out hard modes and obtained an effective 3D action for electrostatic and magnetostatic modes.
- for $p \sim g^2 T$, we have integrated out electrostatic modes as they have a Debye mass $\sim gT$. This leaves us with a magnetostatic Lagrangian.

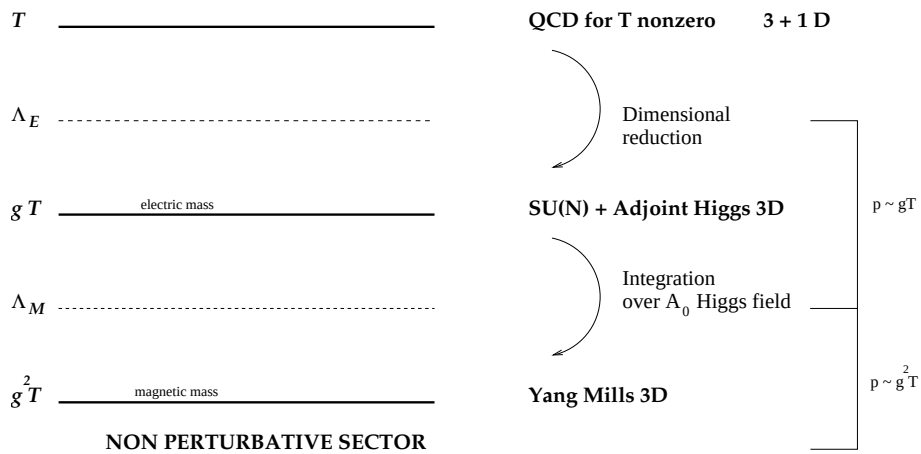


Figure 1: Dimensional reduction at work. Integrating out each physical scale of the plasma will lead to a new effective theory.

As we integrated out non-static modes, the two effectives theories are three-dimensional. This dimensional reduction is the same process as in Kaluza-Klein theories. The procedure is schematically described in Fig. 1.

In a more precise way, we have:

- for the hard modes: eq. (4).
- for the soft modes, after integrating out the heavy modes, we have an $SU(N)$ Yang-Mills + adjoint Higgs effective theory. Its Lagrangian reads:

$$\begin{aligned} \mathcal{L}_E &= Tr(\vec{D}(A)A_0)^2 + m_E^2 Tr A_0^2 + \lambda_E (Tr(A_0^2))^2 + \\ &+ \bar{\lambda}_E \big(Tr(A_0)^4 - \frac{1}{2}(Tr A_0^2)^2\big) + \frac{1}{2} Tr F_{ij}^2 + \delta\mathcal{L}_E. \end{aligned} \tag{5}$$

  with as parameters $g_E(g,T)$, $m_E(g,T)$, etc ... and $\delta\mathcal{L}_E$ represent higher orders operators.
- for the ultra-soft modes, the effective theory is a magnetostatic Yang-Mills:

$$\mathcal{L}_M = \frac{1}{2} Tr F_{ij}^2 + \delta\mathcal{L}_M. \tag{6}$$

  with as parameter $g_M(g_E, m_E$, etc..) and $\delta\mathcal{L}_M$ represent higher orders operators.

All theses Lagrangians are deduced from each other via perturbation theory. That means that they are known to a given order and practically one uses the truncated Lagrangians, for example $\mathcal{L}_M - \delta\mathcal{L}_M$, to do some computation. Of course it is important to know which orders are not taken into account. We will discuss this in the next section.

The technical determination of the magnetostic Lagrangians will be discussed in the next chapter. We can already make some remarks: $\mathcal{L}_M$ is non-perturbative. The theory has a dimensionful coupling constant $g_M^2 \sim g^2 T$. So if one wants to use perturbation theory, the dimensionless expansion parameter is $\frac{g_M^2}{|\vec{p}|}$ which is order 1 for $|\vec{p}| \sim g^2 T$!

Finally, once one has computed the parameters, one has to go to the lattice and use $\mathcal{L}_M$ to determine magnetic properties of the quark-gluon plasma.

## 3 Magnetostatic action in hot QCD

As previously explained we are going to focus our attention on the magnetostatic action $\mathcal{L}_M$. The reason is the following: the non-perturbative terms in the weak coupling expansion of a thermodymamic quantity or an observable come from the magnetostatic Lagrangian. So its study gives us some clues to study numerically and with precision the convergence of the perturbative series at high $T$. Namely, at which degree of precision the magnetostatic Lagrangian has to be known in order to include the major part of non-perturbative effects? The goal of this first part is to determine this Lagrangian up to relative order $g^2$. First we are going to recall explicitely how this magnetostatic Lagrangian is constructed by integrating out the Debye scale in the electrostatic action. Then, as the electrostatic Debye scale is integrated out via perturbation theory, we are going to discuss at which order we make the truncation (i.e. what is the order of $\delta\mathcal{L}_M$) and show the computation of the magnetostatic coupling $g_M$ at two loop order.

### *3.1 From the electrostatic action to the magnetostatic action*

The electrostatic action is determined by integrating out heavy modes in the full QCD Lagrangian, namely gluons with a non-zero Matsubara frequency and quarks. Its domain of validity is for external momenta of order $gT$. Then for momenta of order $g^2T$ one has to integrate the Debye scale. A well-known shortcut is by making a background expansion of the effective potential for the magnetostatic field [8].

Consider $S_M$ the full magnetostatic action containing the $3D$ Yang-Mills and all other higher order terms and $S_E$ the electrostatic action. The static fields in the electrostatic Lagrangian are the massless magnetostatic $A_i$ field and the electrostatic $A_0$ field with mass $m_E$. In order to integrate out the Debye scale, one has to introduce a background field for the magnetostatic field, namely,

$$\vec{A} = \vec{B} + g_E\vec{Q} \tag{7}$$

with $\vec{B}$ the background and $\vec{Q}$ the quantum fluctuations.

Then formally we can construct the magnetostatic action:

$$\exp\left[-\frac{1}{g_M^2}S_M(B_i)\right] = \int DA_0 DQ_i exp[-\frac{1}{g_E^2}S_E(A_0, B_i + g_E Q_i)] \tag{8}$$

where the integration is from external momenta of order $g^2T$ and for diagrams with at least one $A_0$ in the internal loops. This effective action is computed via perturbation theory. That means that one has to use truncation when some computations (namely lattice computations in this case) has to be performed with this magnetostatic action.

### *3.2 Truncated magnetostatic Lagrangian and precision*

Now the aim is to see what is the relative error made by using the truncated magnetostatic Lagrangian.

At this point, it is interesting to recall again that all of the non perturbative part is contained in the magnetostatic Lagrangian. So if one wants to know more about the structure of the non-perturbative terms following a perturbative expansion, for example for the order up to and including $g^6$ for the pressure, its dominant contribution will certainly come from the zero-loop magnetostatic Lagrangian, namely a 3D Yang Mills theory. In fact the whole question is to mesure with lattice simulations the weight of this contribution and also to see if the high order operators in the magnetostatic Lagrangian will be important. This will be the aim of the second part of this paper.

Now, let us take a look at higher order operators. One has to compute the one loop expansion in eq. (8). It gives two operators, namely $\frac{g_E^2 Tr F_{ij}F_{jk}F_{ki}}{m_E^3}$ and $\frac{g_E^2 (D_i F_{ij})^2}{m_E^3}$ [9]. What

is the order of such terms? For example, for the second term the integration of the hard modes have provided that at zero-loop $g_E \sim g^2 T$ and at one-loop $m_E \sim gT$. So, as in this sector, $D \sim g^2 T$, we conclude that $\delta\mathcal{L}_M$ is of relative order $g^3$. The same occurs for the first term.

To put it in a nutshell, to compute corrections of order $g$ to the $3D$ magnetostatic Yang-Mills, the one-loop renormalization of $g_M$ is needed. For the correction of order $g^2$ to the $3D$ magnetostatic Yang-Mills, the two loop renormalization of $g_M$ is needed. Finally for correction of order $g^3$ to the $3D$ magnetostatic Yang-Mills, the three-loop renormalization of $g_M$ but also the first term in $\delta\mathcal{L}_M$ are needed. Now let us go into more details for what is needed for the two-loop renormalization of $g_M$.

### *3.3 The coupling of the magnetostatic Lagrangian*

As we have seen, to determine $\delta\mathcal{L}_M$ at two loop order is to determine its coupling $g_M$ at two loop.

For this we need to compute the two-point function for the background field with at least one $A_0$ into the loop. We calculate the fluctuations around the background in a path integral:

$$\exp -\frac{1}{g_M^2} S_M(B) = \int DA_0 DQ_i \exp \frac{1}{g_E^2}\Big( - S_E - \frac{1}{\xi} Tr(D_i Q_i)^2\Big). \tag{9}$$

We added a general background gauge term. The resulting action $S_M(B)$ is gauge invariant to all loop orders and the renormalization of the coupling is identified from the background field two point function at a momentum $p = O(g^2 T)$:

$$\exp\Big( - \frac{1}{g_M^2} S_M(B)\Big) = \exp\Big( - \frac{1}{g_E^2} S_M(B)\Big)\Big(1 + (F_1^{tr} + F_2^{tr} + ...) S_M(B)\Big). \tag{10}$$

Here $F_i$ is the sum of all Feynman diagrams for the two point function of the background field with $i$ loops and reads:

$$F_i = F_i^{tr}\ (\delta_{lm} p^2 - p_l p_m). \tag{11}$$

This leaves us with the relation, using eq.(10):

$$\frac{1}{g_M^2} = \frac{1}{g_E^2} - F_1^{tr} - F_2^{tr}, \tag{12}$$

with

$$g_E^2 F_1^{tr} = -\frac{1}{48}\frac{g_E^2 N}{\pi m_E} \tag{13}$$

$$g_E^2 F_2^{tr} = -\frac{19}{4608}(\frac{g_E^2 N}{\pi m_E})^2. \tag{14}$$

The next section shows the details of the computation that leads to this result.

## 4 General and systematic method to compute diagramms

The following section aims to recall the systematic methods in order to compute a high order loop expansion. It deals of course with well known facts but it is important to really go into detail in each of these steps in order to see how it efficiently deals with the problem, which is too big to be treated by hand, but simple enough to present intermediate steps explicitely.

First one has to fix the gauge for the magnetostatic field in the Lagrangian. We are going to take the background gauge that insure the gauge independence of our result.

After gauge fixing, our whole electrostatic Lagrangian reads:

$$
\begin{aligned}
\mathcal{L}_E &= Tr(\vec{D}(\vec{B}+g_E\vec{Q})A_0)^2 + m_E^2 Tr A_0^2 + \lambda_E(Tr(A_0^2)) \\
&+ \bar{\lambda}_E\big(Tr(A_0)^4 - \frac{1}{2}(Tr A_0^2)^2\big) && (15)\\
&+ \frac{1}{2}Tr F_{ij}(\vec{B}+g_E\vec{Q})^2 + \frac{1}{\xi}(D_i(\vec{B})Q_i)^2 && (16)\\
&+ \delta\mathcal{L}_E. && (17)
\end{aligned}
$$

Let us recall that the vertices and propagators involving a magnetostatic field are going to be gauge dependent. Here are the Feynman rules with:

- lines for $A_0^a$
- wavy lines for $A_i^a$
- a dot for the background field

They reads:

$$= \frac{\delta_{ab}}{p^2}(\delta_{ij} - (1-\xi)\frac{p_i p_j}{p^2})$$

$$= \frac{\delta_{ab}}{p^2+m^2}$$

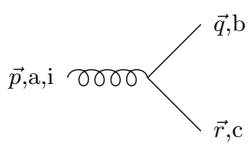


$$= -igf_{abc}(r_i - q_i)$$

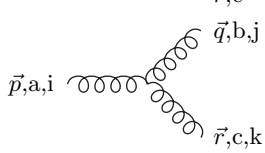


$$= -igf_{abc}(\delta_{ik}(p_j - r_j) + \delta_{jk}(r_i - q_i) + \delta_{ij}(q_k - p_k))$$

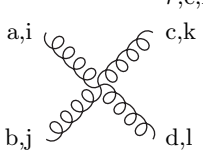


$$
\begin{aligned}
= -g^2(&f_{abe}f_{ecd}(\delta_{ik}\delta_{jl} - \delta_{il}\delta_{jk}) \\
&+ f_{ade}f_{ebc}(\delta_{ij}\delta_{kl} - \delta_{ik}\delta_{jl}) \\
&+ f_{ace}f_{ebd}(\delta_{ij}\delta_{kl} - \delta_{il}\delta_{jk}))
\end{aligned}
$$

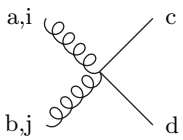


$$= -g^2(f_{ade}f_{ebc} + f_{ace}f_{ebd})\delta_{ij}$$

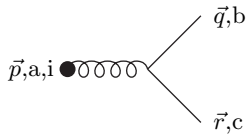


$$= -igf_{abc}(r_i - q_i)$$

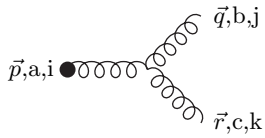


$$\begin{aligned} = -igf_{abc}(&\delta_{ik}(p_j - r_j - \tfrac{q_j}{\xi}) \\ &+\delta_{jk}(r_i - q_i) \\ &+\delta_{ij}(q_k - p_k + \tfrac{r_k}{\xi})) \end{aligned}$$

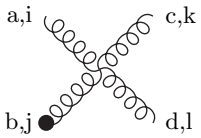


$$\begin{aligned} = -g^2(&f_{abe}f_{ecd}(\delta_{ik}\delta_{jl} - \delta_{il}\delta_{jk}) \\ &+f_{ade}f_{ebc}(\delta_{ij}\delta_{kl} - \delta_{ik}\delta_{jl}) \\ &+f_{ace}f_{ebd}(\delta_{ij}\delta_{kl} - \delta_{il}\delta_{jk})) \end{aligned}$$

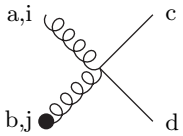


$$= -g^2(f_{ade}f_{ebc} + f_{ace}f_{ebd})\delta_{ij}$$

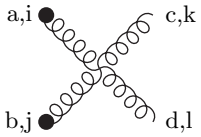


$$\begin{aligned} = -g^2(&f_{abe}f_{ecd}(\delta_{ik}\delta_{jl} - \delta_{il}\delta_{jk} + \delta_{ij}\tfrac{\delta_{kl}}{\xi}) \\ &+f_{ade}f_{ebc}(\delta_{ij}\delta_{kl} - \delta_{ik}\delta_{jl} - \delta_{il}\tfrac{\delta_{jk}}{\xi}) \\ &+f_{ace}f_{ebd}(\delta_{ij} * \delta_{kl} - \delta_{il}\delta_{jk})) \end{aligned}$$

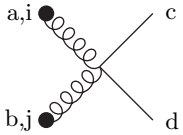


$$= -g^2(f_{ade}f_{ebc} + f_{ace}f_{ebd})\delta_{ij}$$

The two loop graphs to be computed are shown in Fig. 2.

The most naive way to perform the two-loop computation is by following the below vade-mecum.
First:

- contract the indices
- scalarise integrals with no irreducible numerators using FORM [10].

Then:

- Scalarise those which have irreducible numerators (to be defined later)

The whole result can be expressed in terms of 8 scalar integrals . We have to compute them up to $\epsilon$ and expand in terms of $\tilde{p} = \frac{p}{m_E}$. The result has the form:

$$\Pi_{ij} = \Pi(p^2, \xi, d, m^2)(p^2\delta_{ij} - p_i p_j) + C p_i p_j \tag{18}$$

where following our previous convention,

$$lim_{\tilde{p}\to 0}\Pi(p^2, \xi, d, m^2) = F_2^{tr} \tag{19}$$

We have to check:

- the transversality (i.e. $C = 0$)
- gauge independence
- U.V. convergence
- I.R. convergence

At this point graphs 8,11,12,13,14 are zero in dimensional regularisation due to the presence of a massless loop. Diagrams 15 and 16 are one-loop diagrams due to the renormalization of the gauge parameter [8].

The main body of the problem is to express the whole two-loop graphs in term of scalar integrals tabulated in the literature.

## 5 Scalarisation, transversality and the two loop renormalisation

### *5.1 Scalarization*

The key point of the computation is to go from a set of integrals with momenta in the numerator to a set of "master integrals" of a few scalar integrals (8 here) to compute. We are going here to review the two methods of scalarisation that had been used in our two-loop computation. These two methods are then implemented in the Mathematica routine TARCER [11]. They consist of kinematical scalarisation on one hand and in a identity based on integration by parts on the other hand.

Indeed, as our vertices are vectorial, after their contraction with propagators, we obtain for each graph the integral over internal momenta of a product of propagators times a numerator. The goal is then to cancel all the terms in the numerator with propagators. At first sight, a natural way to do this is the so-called "kinematical scalarization". It consists of writing the scalar products of momenta in the numerator as a combination of propagators.
Let us take an example.
Let $q$ and $r$ be the internal momenta, $2q.r$ can be written as $-((q-r)^2+m^2)+(r^2+m^2)+(q^2+m^2)-m^2$. We see here that two situations appear. If all the terms in the rewriting of numerators cancel with the propagators, a scalar integral will remain. This is what we call a reducible integral. If it is not the case, i.e. if a term in the numerator is not present in the denominator, the method fails. This is what we call a irreducible integral. For this

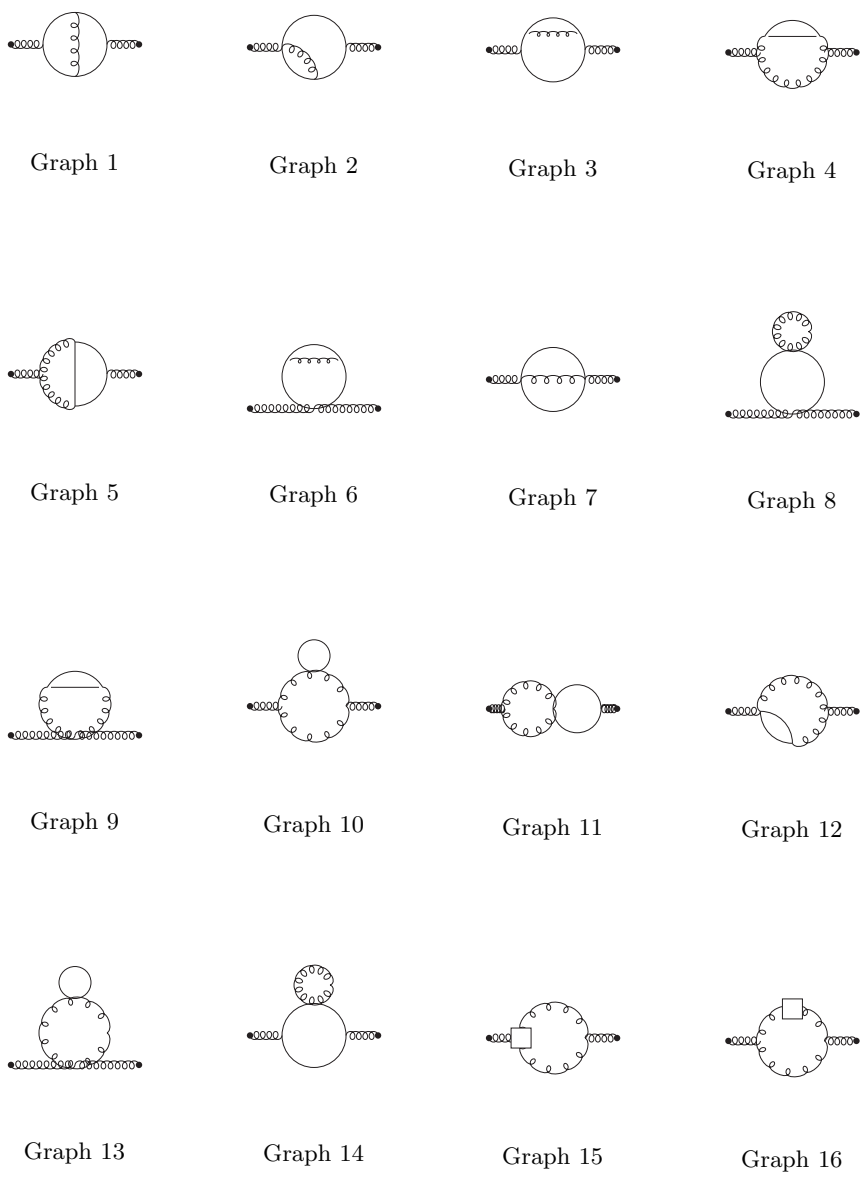


Figure 2: Two-loop Feynman graphs for the background two-point function. The boxes in 15 and 16 represent the one-loop renormalisation of the gauge parameter.

latter, an other algorithm must be used [13 12]. Its non trivial part relies on the following identity [13 12]:

$$\prod_{i=1}^{L} \int d^d k_i \frac{\partial}{\partial k_{ri}} \left\{ R_{\{i\}}\left(\{k\},\{q\}\right) \prod_{j=1}^{N} P^{\nu_j}_{\overline{k}_j, m_j} \right\} \equiv 0 \tag{20}$$

where R is a polynomial function of internal and external momenta, L the number of loops in the diagram and P are the various propagators power $\nu_j$ in the loop.

Those rules have been implemented in TARCER [11]. We first use it in order to demonstrate the transversality of our result. The integral to appear are ( with $d = 3 - 2\epsilon$):

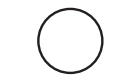

$$= \int \frac{d^d q}{(2\pi)^3} \frac{1}{q^2+m_E^2}$$

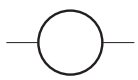

$$= \int \frac{d^d q}{(2\pi)^3} \frac{1}{q^2+m_E^2} \frac{1}{(p+q)^2+m_E^2}$$

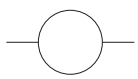

$$= \int \frac{d^d q}{(2\pi)^3} \frac{1}{q^2} \frac{1}{(p+q)^2}$$

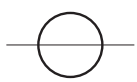

$$= \int\int \frac{d^d q}{(2\pi)^3} \frac{d^d r}{(2\pi)^3} \frac{1}{q^2+m_E^2} \frac{1}{(p+r)^2+m_E^2} \frac{1}{(q-r)^2}$$

$$= \int\int \frac{d^d q}{(2\pi)^3} \frac{d^d r}{(2\pi)^3} \frac{1}{q^2+m_E^2} \frac{1}{r^2+m_E^2} \frac{1}{(q-r)^2}$$

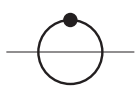

$$= \int\int \frac{d^d q}{(2\pi)^3} \frac{d^d r}{(2\pi)^3} \frac{1}{(q^2+m_E^2)^2} \frac{1}{r^2+m_E^2} \frac{1}{(q-r)^2}$$

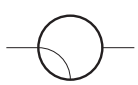

$$= \int\int \frac{d^d q}{(2\pi)^3} \frac{d^d r}{(2\pi)^3} \frac{1}{((q+p)^2+m_E^2)^2} \frac{1}{r^2+m_E^2} \frac{1}{(q-r)^2}$$

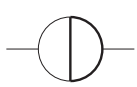

$$= \int\int \frac{d^d q}{(2\pi)^3} \frac{d^d r}{(2\pi)^3} \frac{1}{q^2} \frac{1}{r^2+m_E^2} \frac{1}{(q-r)^2+m_E^2} \frac{1}{(q+p)^2} \frac{1}{(r+p)^2+m_E^2}$$

Their values are given in Appendix 1.

### *5.2 Transversality for any dimension d*

The goal of this section is to check that our result is transverse. This is due to the fact that we compute a self energy using the background method. Before presenting the result, it must be noticed that only the scalarisation process is necessary to prove this. Indeed , one need not to express the master integrals in terms of external momenta, even not to specify the dimension of space. So our result is general. Let us write

$$\tilde{C} = p_i \Pi_{ij} p_j = p^4 C \tag{21}$$

and check that C is zero.

After scalarisation, all the non transverse component can be expressed in terms of three master integrals. These master integrals are tabulated in Appendix 1. As defined in the last subsection, the propagators and vertices are all scalars . Thin lines represent massless propagators and bold line represent massive propagators of mass $m_E$. For each diagram, the result is given in Appendix 2 in terms of the master integrals. Here is the result for the first graph.

$\tilde{C}_1 =$

$$- \quad \frac{d - d^2 + 6\xi - 5d\xi + d^2\xi}{12(-3+d)} ( \quad )^2 +$$

$$- \quad \frac{-24m^2 + 34dm^2 - 10d^2m^2 - 2p^2 + 3dp^2}{12(-2+d)}$$

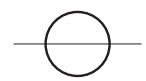

$$- \quad \frac{-d^2p^2 60m^2\xi - 50dm^2\xi + 10d^2m^2\xi}{12(-2+d)}$$

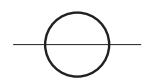

$$- \quad \frac{10p^2\xi - 7dp^2\xi + d^2p^2\xi}{12(-2+d)}$$

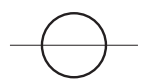

$$- \quad \frac{m^2(4m^2 + p^2)(1 - d - 2\xi + d\xi)}{3(-2+d)}$$

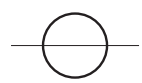

(22)

What we have learnt is that, whereas the whole result is transverse, individuals graphs are not. Moreover, the process of scalarization is sufficient to show explicitely transversality. It will not be the case to show gauge independance of the coupling, where the expressions of master integrals are needed.

When all non transverse contributions are summed up, then the whole result is 0 (see Appendix 2). The latter of course is true for any dimension.

### *5.3 Scalarisation of the transverse part*

Now that we have demonstrated that our result is transverse, we want to compute the renormalisation of the coupling. We have to scalarize the transverse part. The complexity of the following computation is due to the presence of a general gauge parameter $\xi$ in the Lagrangian, that is reflected by the gauge dependence of the magnetic gluon propagator. But also, due to the presence of a magnetic background, to the gauge dependence of the vertices. Let us call $Fi_2$ the value of a two-loop graph contracted with $\delta_{ij}$. We have

$$\sum_i Fi_2 = p^2 F_2^{tr} \tag{23}$$

For the first graph, the result reads:

$F1_2 =$

$$-\quad \frac{48m^4-96dm^4+60d^2m^4}{12(-4+d)(-3+d)m^2p^2(4m^2+p^2)}\Big($$ $$\Big)^2$$

$$-\quad \frac{-12d^3m^4+36m^2p^2-50dm^2p^2}{12(-4+d)(-3+d)m^2p^2(4m^2+p^2)}\Big($$ $$\Big)^2$$

$$-\quad \frac{17d^2m^2p^2-3d^3m^2p^2+12p^4-6dp^4}{12(-4+d)(-3+d)m^2p^2(4m^2+p^2)}\Big($$ $$\Big)^2$$

$$-\quad \frac{-144m^4\xi+192dm^4\xi-84d^2m^4\xi}{12(-4+d)(-3+d)m^2p^2(4m^2+p^2)}\Big($$ $$\Big)^2$$

$$-\quad \frac{12d^3m^4\xi-36m^2p^2\xi+48dm^2p^2\xi}{12(-4+d)(-3+d)m^2p^2(4m^2+p^2)}\Big($$ $$\Big)^2$$

$$-\quad \frac{-21d^2m^2p^2\xi+3d^3m^2p^2\xi}{12(-4+d)(-3+d)m^2p^2(4m^2+p^2)}\Big($$ $$\Big)^2$$

$$-\quad \frac{4m^2-2p^2+dp^2}{2(-4+d)(-3+d)m^2}$$

$$-\quad \frac{2m^2+p^2}{2(-4+d)}\Big($$ 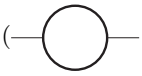 $$\Big)^2$$

$$-\quad \frac{384m^4-720dm^4+408d^2m^4-72d^3m^4}{12(-4+d)(-2+d)p^2(4m^2+p^2)}$$ 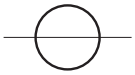

$$-\quad \frac{144m^2p^2-200dm^2p^2+134d^2m^2p^2}{12(-4+d)(-2+d)p^2(4m^2+p^2)}$$ 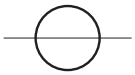

$$-\quad \frac{-30d^3m^2p^2-32p^4+18dp^4+5d^2p^4-3d^3p^4}{12(-4+d)(-2+d)p^2(4m^2+p^2)}$$ 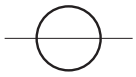

$$-\quad \frac{-1152m^4\xi+1392dm^4\xi-552d^2m^4\xi+72d^3m^4\xi}{12(-4+d)(-2+d)p^2(4m^2+p^2)}$$ 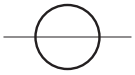

$$-\quad \frac{-480m^2p^2\xi+564dm^2p^2\xi-222d^2m^2p^2\xi}{12(-4+d)(-2+d)p^2(4m^2+p^2)}$$ 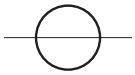

$$
\begin{aligned}
&- \quad \frac{30d^3m^2p^2\xi - 48p^4\xi + 54dp^4\xi - 21d^2p^4\xi}{12(-4+d)(-2+d)p^2(4m^2+p^2)} \\
&- \quad \frac{3d^3p^4\xi}{12(-4+d)(-2+d)p^2(4m^2+p^2)} \\
&- \quad \frac{36m^4 - 66dm^4 + 36d^2m^4 - 6d^3m^4 - 11dm^2p^2}{3(-4+d)(-3+d)(-2+d)p^2} \\
&- \quad \frac{14d^2m^2p^2 - 3d^3m^2p^2 - 6p^4 + 3dp^4}{3(-4+d)(-3+d)(-2+d)p^2} \\
&- \quad \frac{-108m^4\xi + 126dm^4\xi - 48d^2m^4\xi + 6d^3m^4\xi}{3(-4+d)(-3+d)(-2+d)p^2} \\
&- \quad \frac{-36m^2p^2\xi + 48dm^2p^2\xi - 21d^2m^2p^2\xi + 3d^3m^2p^2\xi}{3(-4+d)(-3+d)(-2+d)p^2} \\
&+ \quad \frac{(-1+d)p^2(2m^2+3p^2)}{12(-1+d)m^2p^2(4m^2+p^2)}(\quad)^2 \\
&- \quad \frac{(-1+d)p^2}{4(-1+d)m^2} \\
&+ \quad \frac{(-1+d)p^2}{2(-1+d)(4m^2+p^2)} \\
&- \quad \frac{(-1+d)p^2(-12m^4 + 4dm^4 - 14m^2p^2 + 4dm^2p^2)}{12(-2+d)(-1+d)m^2p^2(4m^2+p^2)} \\
&- \quad \frac{(-1+d)p^2(2m^2+3p^2)}{6(-2+d)(-1+d)p^2} \\
&- \quad \frac{(-1+d)p^2}{2(-1+d)}
\end{aligned}
\tag{24}
$$

Considering the example above, further general remarks can be made. First, compared with the non-transverse part of the first graph that has been shown previously, the transverse part involves more master integrals and is a little bit more complicated. Moreover, in the scalarisation process, some poles in $\epsilon$ appear. They will of course cancel, witnessing U.V. convergence. But attention has to be paid when one has to compute the final

| Graph no | $p^2 F_2^{tr}$ |
|---|---|
| 1 | $-\frac{\tilde{p}^2(29+24\xi)}{9216\pi^2}+\frac{1+\xi+\epsilon(2+\xi-4(1+\xi)\log(2))+4\epsilon(1+\xi)\log(\frac{\bar{\mu}}{m})}{128\epsilon\pi^2}$ |
| 2 | $\frac{\tilde{p}^2(20+6\xi)}{1536\pi^2}-\frac{3(2+\xi-2\epsilon(-1+\xi(-1+\log(4))+\log(16))+4\epsilon(2+\xi)\log(\frac{\bar{\mu}}{m})))}{128\epsilon\pi^2}$ |
| 3 | $\frac{\tilde{p}^2(-43+12\xi)}{4608\pi^2}+\frac{4+\epsilon(1+\xi-16\log(2))+16\epsilon\log(\frac{\bar{\mu}}{m})}{64\epsilon\pi^2}$ |
| 4 | $\frac{-2-\xi}{32\tilde{p}\pi}-\frac{\tilde{p}(15+\xi))}{1536\pi}+\frac{\tilde{p}^2(13+2\xi)}{3072\pi^2}-\frac{3(1+\xi)^2+4\epsilon(-8+\xi)\xi\log(\frac{\bar{\mu}}{2m})+4\epsilon(3+2\xi(7+\xi))\log(\frac{\bar{\mu}}{2m})}{768\epsilon\pi^2\xi}$ |
| 5 | $\frac{\tilde{p}(15+\xi(4+\xi))}{1536\pi}-\frac{\tilde{p}^2(23+12\xi)}{4608\pi^2}+\frac{2\epsilon+\xi+4\epsilon\xi\log(\frac{\bar{\mu}}{2m})}{128\epsilon\pi^2}$ |
| 6 | $\frac{-3}{(64\epsilon\pi^2)}+\frac{22-24(1+\log(\frac{\bar{\mu}}{2m}))}{128\pi^2}$ |
| 7 | $\frac{6(2+\xi)+\epsilon(12(1+\xi)-\tilde{p}^2(2+\xi))+24\epsilon(2+\xi)\log(\frac{\bar{\mu}}{2m})}{512\epsilon\pi^2}$ |
| 8 | 0 |
| 9 | $\frac{1+2\xi}{256\epsilon\pi^2\xi}+\frac{-2\xi-4(1+2\xi)-4(-1-2\xi)(1+\log(\frac{\bar{\mu}}{2m}))}{256\pi^2\xi}$ |
| 10 | $\frac{16+8\xi}{256\tilde{p}\pi}$ |
| 11 | 0 |
| 12 | 0 |
| 13 | 0 |
| 14 | 0 |
| 15 | $-\frac{\tilde{p}(1+\xi)(4+\xi)}{1536\pi}$ |
| 16 | $\frac{\tilde{p}(2+\xi)}{768\pi}$ |
| sum | $\frac{-19\tilde{p}^2}{4608\pi^2}$ |

Figure 3: Final result for each graph up to $O(\tilde{p}^2)$.

result. Indeed some final parts when $\epsilon \to 0$ are provided by the product of a $\frac{1}{\epsilon}$ coming from scalarization and the first term in $\epsilon$ of a master integral. Indeed not all the master integrals have to be computed up and includind $O(\epsilon)$.

### *5.4 Result*

Once one has computed the master integrals and develop them for $p^2 \ll m_E^2$, the table in Fig. 3 is obtained. So finally

$$\sum_i Fi_2 = p^2 F_2^{tr} = \frac{-19\tilde{p}^2}{4608\pi^2} \tag{25}$$

This result has of course no pole in $\epsilon$, is $\xi$ independant, has no pole in $\tilde{p}$, is $\mu$ independant whereas each graph does not have these properties. This is a really strong check of our computation. Going into more detail will show that this check is robust in the sense that an error in a integral will show up through one of this checks. So the result is simply:

$$g_M^{(2)} = \frac{-19}{4608\pi^2 m_E^2} g_E^4 N^2 \tag{26}$$

Our main result, eq.(14), shows that the smallness of the corrections to the magnetic coupling does persist in two-loop order. In fact, at $2T_c$ the coupling for 3 colours equals [14] $g_E^2 = 2.7$ and the two-loop correction is about a third of the one loop correction (itself about 3 percent).

Our result is of importance in analyzing the purely magnetic quantities, such as the spatial Wilson loop, and the magnetic mass. In particular it is crucial in connecting the lattice results from the magnetic action to those obtained from the electric action, and ultimately to those of four dimensional simulations.

## 6 Spatial Wilson Loop

The goal of this part is to test the applicability of 3D physics at intermediate T.

As has been recalled previously, the non-perturbative part in the weak coupling expansion of an observable comes from its magnetostatic thermal average. The dominant term of this non-perturbative part comes from the $3D$ dimensional Yang-Mills with its coupling computed a zero-loop order. Its next term is a $3D$ dimensional Yang-Mills with its coupling computed a one-loop order. Then a three-dimensional Yang-Mills with its coupling computed a two-loop order. Then the next term is the mix of a three-dimensional Yang-Mills with its coupling computed at three-loop order and higher order operators.

Our actual knowledge of the non-perturbative part is now the 3D Yang-Mills action with its coupling computed at two-loop order. The natural question is: does this precision encompass almost the whole non perturbative contribution to the thermal average of an observable ?

Let us consider an observable which has its dominant contribution from the 3D Yang-Mills sector, unlike the pressure whose dominant contribution is the Stefan-Boltzmann term due to hard modes. That means that at infinite temperature, its thermal average is computed with the zero-loop magnetostatic Lagrangian, namely the three-dimensional Yang-Mills action.

Such an observable is the spatial Wilson loop in the fundamental representation:

$$W(L) = TrP \exp\,(i \oint_L g\vec{A} \cdot d\vec{l}). \tag{27}$$

As $L$ is purely spatial, it measures the magnetic flux in the plasma. The thermal average of this spatial Wilson loop shows area behaviour with a surface tension $\sigma(T)$. As this is a purely magnetic quantity, we expect from dimensional arguments that $\sqrt{\sigma} = cg_M^2$ where $c$ is a nonperturbative proportionality constant. Indeed, as the average of the loop is due to long distance correlations, hard modes will not have any effect on the thermal average. In the same way, for soft modes, we can integrate out the $A_0$ field, which is what we have done in the previous section while constructing $L_M$, as the loop does not depend on $A_0$ ! Finally, we have:

$$\langle W(L)\rangle = \exp -\sigma A(L) = \frac{\int D\vec{A} W(L) \exp -S_M(A)}{\int D\vec{A} \exp -S_M(A)}, \tag{28}$$

and it gives, as $\delta L_M$ is of relative order $g^3$,

$$\sigma(T) = c^2 g_M^4 (1 + O(g^3)). \tag{29}$$

Now the aim is to fit with our formula for $g_M$ the proportionality constant $c$. For that, we have to go to the lattice. We are going to fit $\frac{T}{\sqrt{\sigma}}$ as a function of $\frac{T}{T_c}$. Indeed, $g_M$ is a function of $g_E$ and $m_E$ which are functions of $g$ and $T$. So, for $N = 3$:

$$g_M^{-2} = g^{-2} T^{-1} (1 + \frac{g}{16\pi} + \frac{19g^2}{512\pi^2}) \tag{30}$$

with

$$g^{-2} = \frac{11}{8\pi^2}(Log(\frac{T}{T_c}) + Log(\frac{T_c}{\Lambda_{\overline{MS}}}) + 1.90835...). \tag{31}$$

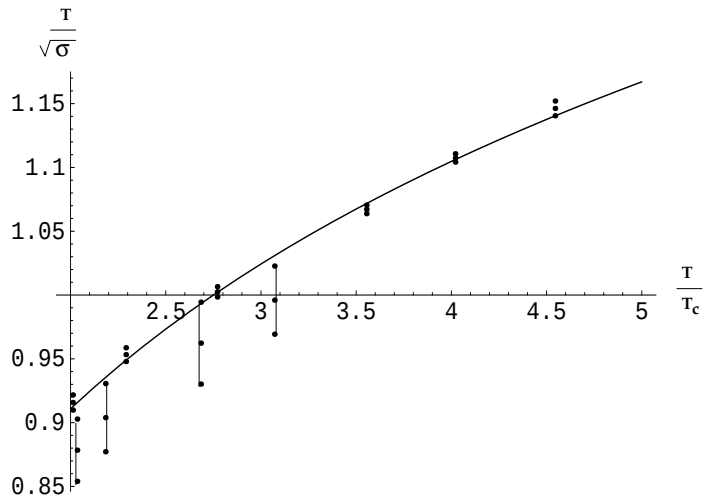


Figure 4: Plot of $\frac{T}{\sqrt{\sigma}}$ versus $\frac{T}{T_c}$ and fit with our two-loop formula. Each of the 10 points is shown with its error bar.

The $\mu$ dependance will be discussed in next section. So thanks to these formulas, one can fit $\frac{T}{\sqrt{\sigma}}$ versus $\frac{T}{T_c}$ in order to determin $c$ and $\frac{T_c}{\Lambda_{\overline{MS}}}$. Data points for the $SU(3)$ spatial string tension has been taken from [15,16] for $T > 2T_c$. So we have 10 points. The fit is shown in fig 4.

The fit gives:

$$\frac{T_c}{\Lambda_{\overline{MS}}} = 1.78(12) \tag{32}$$

$$c = 0.505(11). \tag{33}$$

In order to estimate the error in our fit, we have plotted for those 10 points the confidence levels taken from the $\chi^2$ distribution. Compared with the results in the literature our values are incompatible with them.

Then we have also fitted data with $T > 2.5T_c$. This leaves us with 6 points. We obtained

$$\frac{T_c}{\Lambda_{\overline{MS}}} = 1.57(20) \tag{34}$$

$$c = 0.488(18) \tag{35}$$

We have plotted for the 4 more precise of those 6 points the 95 percent confidence level contour taken from the $\chi^2$ distribution in Fig. 5. Let us draw our conclusions.

Despite the fact that the region of confidence is larger, the value of $\frac{T_c}{\Lambda_{\overline{MS}}}$ and c is still incompatible with refs. [17,18,19]. To see compatibility one obviously needs string data for higher $T$. It might also be recommendable to use other Monte Carlo updates, like the one described in ref. [20], which is a version of the Lüscher-Weisz algorithm [21].

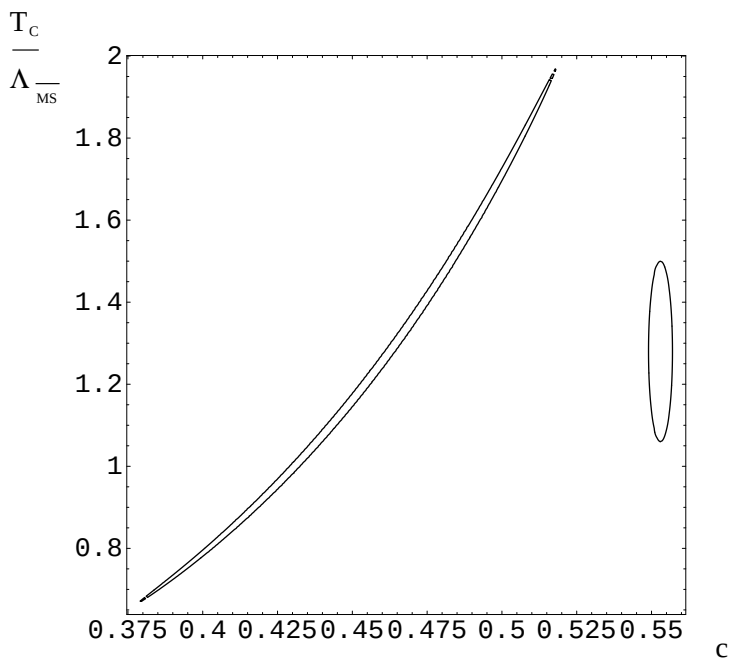


Figure 5: Plot of various confidence levels in the plane c- $\frac{T_c}{\Lambda_{\overline{MS}}}$ for the 4 data points with the smallest error bar. The widespread ellipse on the left delimits the 95 percent confidence level for the parameters. The central values are $c = 0.481$ and $\frac{T_c}{\Lambda_{\overline{MS}}} = 1.27$. The ellipse on the r.h.s. represents the actual values for these parameters from the literature [23,17,18].

### *6.1 Renormalisation scale dependence*

In the previous section, we have taken implicitely, as renormalisation scale, the one that cancels the one loop renormalisation due to hard modes of the electric coupling, namely $\tilde{\mu_T} = \mu_T = 4\pi T e^{-\gamma_E} e^{\frac{-1}{11}}$ [22].

This $\mu$ dependence appears explicitely when one tries to express the magnetic coupling $g_M$ as a function of the QCD coupling $g$. In fact the renormalization scale will appear in two ways. The first is through the renormalization of the QCD coupling, and the second is in the expression of $g_E$ as a function of $g$.

Namely, for a pure gauge theory, the electrostatic coupling reads

$$g_E^2 = g^2(\mu)T(1 + \frac{11N}{24}(Log(\frac{\mu}{\tilde{\mu}_T})) \tag{36}$$

where

$$g^2(\mu) = \frac{24\pi^2}{11Nln(\mu/\Lambda_{\overline{MS}})} \tag{37}$$

If one combines those two equations, evaluating in $\mu = \tilde{\mu}_T + \delta\mu$, one finds that, in our case with no fermions, the first term in $\delta\mu$ will disappear when one expand $g_E^2$ near $\mu = \tilde{\mu}_T$.

### *6.2 Conclusion*

We have seen that we have not yet captured the full $4D$ physics with our truncation. That means that higher order terms are needed to make the link. This has been done recently by considering the two loop renormalization of $g_E$ [24]. The conclusion, also with the fact that we need more lattice data, is that at the temperatures that we have considered, perturbative and non-perturbative effects are both important. The next step is to compute the magnetostatic Lagrangian at higher order, determining for example the leading higher dimensional operators. This will be the purpose of a forthcoming paper [9]

**Acknowledgment**

I thank Chris Korthals Altes for his help throughout my work. I acknowledge the help of Mikko Laine and York Schröder for very useful and stimulating advice. I thank the DAAD and the University of Bielefeld for financial support.

**Appendix 1: Scalar Integrals**

In this appendix, we compute the master integrals that appear in the non-transverse part. The computation is carried out for $d = 3 - 2\epsilon$. For $\epsilon = 0$, these integrals have been tabulated in Ref. [25]. For some of them, when a $\frac{1}{\epsilon}$ appears in the process of scalarisation for one of the Feynman graphs, we have to compute the first term in the $\epsilon$ expansion. This has been done using the same techniques as in [25]. At the end, one has not to forget that we are only interested in the result for $p^2 \ll m_E^2$ where $p$ is the external momentum. We have used the same notations as in Ref. [25], namely, the measure of integration is $\int \frac{d\vec{l}}{(2\pi)^d}$ and thin lines represent massless propagators and bold line represent massive propagators of mass $m_E$.

$$= -\frac{m_E}{4\pi}(1+2\epsilon)(1+\log\frac{\bar{\mu}}{2m_E})) + O(\epsilon^2)$$

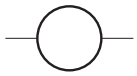

$$= \frac{ArcTan\frac{p}{2m_E}}{4p\pi} - (2\epsilon)R_1(p^2) + O(\epsilon^2)$$

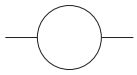

$$= \frac{1}{8p} + O(\epsilon)$$

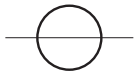

$$= \frac{1}{(4\pi)^2}(\frac{1}{4\epsilon} + 3/2 - 2m_E\frac{ArcTan\frac{p}{2m_E}}{p}$$

$$+\frac{Log\frac{\bar{\mu}^2}{p^2+4m_E^2}}{2}) + O(\epsilon)$$

$$= \frac{1}{(4\pi)^2}(\frac{1}{4\epsilon} + 1/2 + Log\frac{\bar{\mu}}{2m_E}) + O(\epsilon)$$

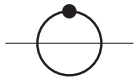

$$= \frac{ArcTan\frac{p}{2m_E}}{(4\pi)^2}\frac{1}{2m_E p} + (-2\epsilon)R_2(p^2) + O(\epsilon^2)$$

For the two following master integrals, only the part in $\epsilon = 0$ is required. Moreover, they have been developed in $\tilde{p} = \frac{p}{m_E}$.

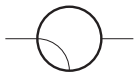

$$= \frac{1}{(4m^2)}\frac{1}{(4\pi)^2} + O(p^2)$$

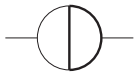

$$= \frac{1}{256\pi p^2 m_E^2} - \frac{1}{256\pi^2 m_E^4} + O(p^2)$$

Then, the computation contained in the main body of this paper (see Appendix 3) shows that we have to determine the first term in $\epsilon$ contained in two scalar integrals. Namely:

$$R_1(p^2) = \frac{-1}{2}\frac{Log\frac{\bar{\mu}^2}{(2m_E)^2}}{8\pi m_E} + p^2\frac{-Log\frac{\bar{\mu}^2}{(2m_E)^2} - 2}{96m_E^3\pi} + O(p^4) \tag{38}$$

$$R_2(p^2) = \frac{1 + Log\frac{\bar{\mu}^2}{(2m_E)^2}}{32m_E^2\pi^2} + p^2\frac{-17 - 12Log\frac{\bar{\mu}}{(2m_E)}}{4608m_E^4\pi^2} + O(p^4) \tag{39}$$

**Appendix 2**

In this Appendix, the non-transverse part, contracted with $p_i p_j$ is computed for each graph.

$\tilde{C}_1 =$

$$- \frac{d - d^2 + 6\xi - 5d\xi + d^2\xi}{12(-3+d)} ( \quad )^2 +$$

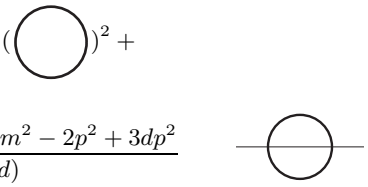

$$- \frac{-24m^2 + 34dm^2 - 10d^2m^2 - 2p^2 + 3dp^2}{12(-2+d)}$$

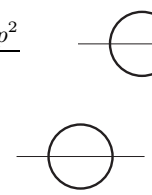

$$- \frac{-d^2p^2 60m^2\xi - 50dm^2\xi + 10d^2m^2\xi}{12(-2+d)}$$

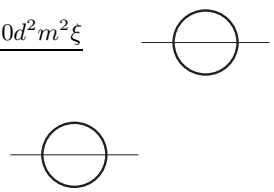

$$- \frac{10p^2\xi - 7dp^2\xi + d^2p^2\xi}{12(-2+d)}$$

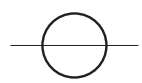

$$- \frac{m^2(4m^2+p^2)(1-d-2\xi+d\xi)}{3(-2+d)}$$

(40)

$\tilde{C}_2 =$

$$- \frac{(-1+d)(-1+\xi)}{4} ( \quad )^2$$

$$+ \frac{-3m^2 + 4dm^2 - d^2m^2 - 2p^2 + 3dp^2 - d^2p^2 + 3m^2\xi}{2(-2+d)}$$

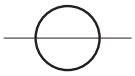

$$+ \frac{-4dm^2\xi + d^2m^2\xi + 8p^2\xi - 6dp^2\xi + d^2p^2\xi}{2(-2+d)}$$

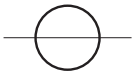

$$+ \frac{(-1+d)m^2(4m^2+p^2)(-1+\xi)}{2(-2+d)}$$

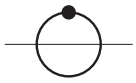

(41)

$\tilde{C}_3 =$

$$+ \frac{-6m^2 + 10dm^2 - 4d^2m^2 - 6p^2 + 9dp^2}{12(-3+d)m^2} ( \quad )^2$$

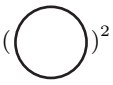

$$+ \frac{-3d^2p^2 + 18m^2\xi - 18dm^2\xi + 4d^2m^2\xi}{12(-3+d)m^2} ( \quad )^2$$

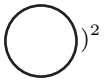

$$+ \quad \frac{(-18m^2+8dm^2+2p^2-dp^2)(1-d-3\xi+d\xi)}{6(-2+d)}$$ 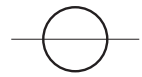

$$+ \quad \frac{m^2(4m^2+p^2)(1-d-3\xi+d\xi)}{3(-2+d)}$$ 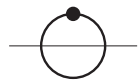

(42)

$\tilde{C}_4 =$

$$+ \quad \frac{-6p^2+9dp^2-3d^2p^2+15dm^2\xi-33d^2m^2\xi}{24(-5+d)(-3+d)dm^2\xi}($$ $)^2$

$$+ \quad \frac{21d^3m^2\xi-3d^4m^2\xi+6p^2\xi-15dp^2\xi}{24(-5+d)(-3+d)dm^2\xi}($$ $)^2$

$$+ \quad \frac{12d^2p^2\xi-3d^3p^2\xi-75dm^2\xi^2}{24(-5+d)(-3+d)dm^2\xi}($$ $)^2$

$$+ \quad \frac{85d^2m^2\xi^2-29d^3m^2\xi^2+3d^4m^2\xi^2}{24(-5+d)(-3+d)dm^2\xi)}$$ $)^2$

$$+ \quad \frac{-21m^2+30dm^2-9d^2m^2+57m^2\xi-46dm^2\xi}{12(-2+d)}$$ 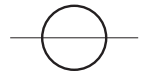

$$+ \quad \frac{9d^2m^2\xi+2p^2\xi-dp^2\xi}{12(-2+d)}$$ 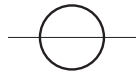

$$+ \quad \frac{m^2(4m^2+p^2)(3-3d-7\xi+3d\xi)}{12(-2+d)}$$ 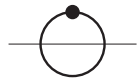

(43)

$\tilde{C}_5 =$

$$- \quad \frac{-3+6d-3d^2+15\xi-14d\xi+3d^2\xi}{12(-3+d)}($$ 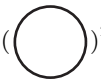 $)^2$

$$- \quad \frac{-21m^2+30dm^2-9d^2m^2+57m^2\xi}{6(-2+d)}$$ 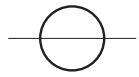

$$- \quad \frac{-46dm^2\xi+9d^2m^2\xi+2p^2\xi-dp^2\xi}{6(-2+d)}$$ 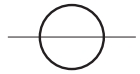

$$- \quad \frac{m^2(4m^2+p^2)(3-3d-7\xi+3d\xi)}{6(-2+d)}$$ 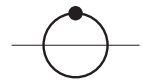

(44)

$\tilde{C}_6 =$

$$+ \quad \frac{(-2+d)(-1+d)p^2}{4(-3+d)m^2}($$ $$)^2$$

(45)

$\tilde{C}_7 =$

$$+ \quad \frac{(-1+d)(-1+\xi)}{8}($$ $$)^2$$

$$- \quad \frac{-3m^2+4dm^2-d^2m^2-2p^2}{4(-2+d)}$$ 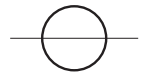

$$- \quad \frac{3dp^2-d^2p^2+3m^2\xi-4dm^2\xi+d^2m^2\xi}{4(-2+d)}$$ 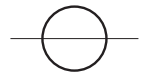

$$- \quad \frac{8p^2\xi-6dp^2\xi+d^2p^2\xi}{4(-2+d)}$$ 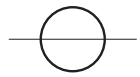

$$- \quad \frac{(-1+d)m^2(4m^2+p^2)(-1+\xi)}{(4(-2+d)}$$ 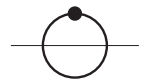

(46)

$\tilde{C}_9 =$

$$\frac{(-2+d)(-1+d)p^2(1-\xi+d\xi)}{8(-5+d)(-3+d)dm^2\xi}($$ $$)^2$$ (47)

$\tilde{C}_{10} = 0$
$\tilde{C}_{15} = 0$
$\tilde{C}_{16} = 0$

When all the contributions are summed up, the result is zero.

**Appendix 3**

In this section the expression of the transverse part of each graph is given in terms of the 8 scalar integrals:

$F1_2 =$

$$- \frac{48m^4 - 96dm^4 + 60d^2m^4}{12(-4+d)(-3+d)m^2p^2(4m^2+p^2)} ( \quad )^2$$

$$- \frac{-12d^3m^4 + 36m^2p^2 - 50dm^2p^2}{12(-4+d)(-3+d)m^2p^2(4m^2+p^2)} ( \quad )^2$$

$$- \frac{17d^2m^2p^2 - 3d^3m^2p^2 + 12p^4 - 6dp^4}{12(-4+d)(-3+d)m^2p^2(4m^2+p^2)} ( \quad )^2$$

$$- \frac{-144m^4\xi + 192dm^4\xi - 84d^2m^4\xi}{12(-4+d)(-3+d)m^2p^2(4m^2+p^2)} ( \quad )^2$$

$$- \frac{12d^3m^4\xi - 36m^2p^2\xi + 48dm^2p^2\xi}{12(-4+d)(-3+d)m^2p^2(4m^2+p^2)} ( \quad )^2$$

$$- \frac{-21d^2m^2p^2\xi + 3d^3m^2p^2\xi}{12(-4+d)(-3+d)m^2p^2(4m^2+p^2)} ( \quad )^2$$

$$- \frac{4m^2 - 2p^2 + dp^2}{2(-4+d)(-3+d)m^2}$$

$$- \frac{2m^2 + p^2}{2(-4+d)} ( \quad )^2$$

$$- \frac{384m^4 - 720dm^4 + 408d^2m^4 - 72d^3m^4}{12(-4+d)(-2+d)p^2(4m^2+p^2)}$$

$$- \frac{144m^2p^2 - 200dm^2p^2 + 134d^2m^2p^2}{12(-4+d)(-2+d)p^2(4m^2+p^2)}$$

$$- \frac{-30d^3m^2p^2 - 32p^4 + 18dp^4 + 5d^2p^4 - 3d^3p^4}{12(-4+d)(-2+d)p^2(4m^2+p^2)}$$

$$- \frac{-1152m^4\xi + 1392dm^4\xi - 552d^2m^4\xi + 72d^3m^4\xi}{12(-4+d)(-2+d)p^2(4m^2+p^2)}$$

$$- \frac{-480m^2p^2\xi + 564dm^2p^2\xi - 222d^2m^2p^2\xi}{12(-4+d)(-2+d)p^2(4m^2+p^2)}$$ 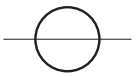

$$- \frac{30d^3m^2p^2\xi - 48p^4\xi + 54dp^4\xi - 21d^2p^4\xi}{12(-4+d)(-2+d)p^2(4m^2+p^2)}$$ 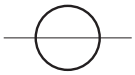

$$- \frac{3d^3p^4\xi}{12(-4+d)(-2+d)p^2(4m^2+p^2)}$$ 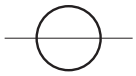

$$- \frac{36m^4 - 66dm^4 + 36d^2m^4 - 6d^3m^4 - 11dm^2p^2}{3(-4+d)(-3+d)(-2+d)p^2}$$ 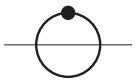

$$- \frac{14d^2m^2p^2 - 3d^3m^2p^2 - 6p^4 + 3dp^4}{3(-4+d)(-3+d)(-2+d)p^2}$$ 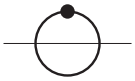

$$- \frac{-108m^4\xi + 126dm^4\xi - 48d^2m^4\xi + 6d^3m^4\xi}{3(-4+d)(-3+d)(-2+d)p^2}$$ 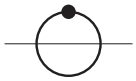

$$- \frac{-36m^2p^2\xi + 48dm^2p^2\xi - 21d^2m^2p^2\xi + 3d^3m^2p^2\xi}{3(-4+d)(-3+d)(-2+d)p^2}$$ 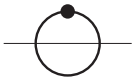

$$+ \frac{(-1+d)p^2(2m^2+3p^2)}{12(-1+d)m^2p^2(4m^2+p^2)}\Big($$ 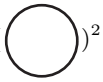 $$\Big)^2$$

$$- \frac{(-1+d)p^2}{4(-1+d)m^2}$$ 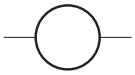

$$+ \frac{(-1+d)p^2}{2(-1+d)(4m^2+p^2)}$$

$$- \frac{(-1+d)p^2(-12m^4 + 4dm^4 - 14m^2p^2 + 4dm^2p^2)}{12(-2+d)(-1+d)m^2p^2(4m^2+p^2)}$$ 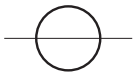

$$- \frac{(-1+d)p^2(2m^2+3p^2)}{6(-2+d)(-1+d)p^2}$$ 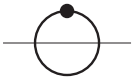

$$- \frac{(-1+d)p^2}{2(-1+d)}$$ 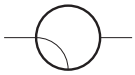

(48)

$F2_2 =$

$+ \quad \frac{-18m^2 + 14dm^2 - 6p^2 + 3dp^2}{8(-3+d)m^2(4m^2+p^2)}($ $)^2$

$- \quad \frac{3(-4m^2 + 4dm^2 - 2p^2 + dp^2)}{8(-3+d)m^2}$ 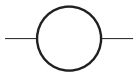

$- \quad \frac{-18m^2 + 14dm^2 - 10p^2 + 5dp^2 - 48m^2\xi + 24dm^2\xi - 12p^2\xi + 6dp^2\xi}{4(-2+d)(4m^2+p^2)}$ 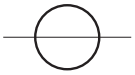

$- \quad \frac{-18m^2 + 14dm^2 - 6p^2 + 3dp^2}{4(-3+d)(-2+d)}$ 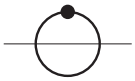

$+ \quad \frac{3(-1+d)p^2(2m^2+3p^2)}{12(-1+d)m^2p^2(4m^2+p^2)2}($ $)^2$

$- \quad \frac{3(-1+d)p^2}{4(-1+d)2m^2}$ 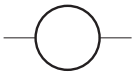

$+ \quad \frac{3(-1+d)p^2}{2(-1+d)2(4m^2+p^2)}$

$- \quad \frac{3(-1+d)p^2(-12m^4 + 4dm^4 - 14m^2p^2 + 4dm^2p^2)}{12(-2+d)2(-1+d)m^2p^2(4m^2+p^2)}$ 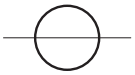

$- \quad \frac{3(-1+d)p^2(2m^2+3p^2)}{6(-2+d)2(-1+d)p^2}$ 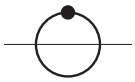

$- \quad \frac{3(-1+d)p^2}{2(-1+d)2}$ 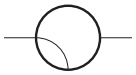

(49)

$F3_2 =$

$+ \quad \frac{(-2+d)(-4m^2 + 6dm^2 - 2d^2m^2 - 4p^2 + 5dp^2 - d^2p^2 + 12m^2\xi - 10dm^2\xi + 2d^2m^2\xi)}{(4(-4+d)(-3+d)m^2p^2}($ $)^2$

$+ \quad \frac{(-1+d)^2}{2(-3+d)}$ 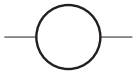

$$+ \quad \frac{(-16m^2+6dm^2+dp^2)(1-d-3\xi+d\xi)}{2(-4+d)p^2}$$ 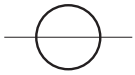

$$+ \quad \frac{2m^2(-6m^2+2dm^2-2p^2+dp^2)(1-d-3\xi+d\xi)}{(-4+d)(-3+d)p^2}$$ 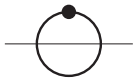

(50)

$F4_2 =$

$$+ \quad \frac{(-2+d)(240m^2p^2-240dm^2p^2-20160m^4\xi)}{1920(-5+d)(-3+d)m^4p^2\xi}($$ 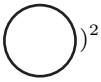 $)^2$

$$+ \quad \frac{(-2+d)(+52832dm^4\xi-37440d^2m^4\xi+9696d^3m^4\xi)}{1920(-5+d)(-3+d)m^4p^2\xi}($$ 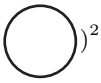 $)^2$

$$+ \quad \frac{(-2+d)(-832d^4m^4\xi+1864m^2p^2\xi-4008dm^2p^2\xi)}{1920(-5+d)(-3+d)m^4p^2\xi}($$ 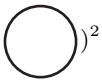 $)^2$

$$+ \quad \frac{(-2+d)(+3352d^2m^2p^2\xi-1208d^3m^2p^2\xi+128d^4m^2p^2\xi)}{1920(-5+d)(-3+d)m^4p^2\xi}($$ 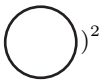 $)^2$

$$+ \quad \frac{(-2+d)(-420p^4\xi+509dp^4\xi-225d^2p^4\xi+43d^3p^4\xi)}{1920(-5+d)(-3+d)m^4p^2\xi}($$ 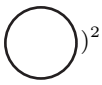 $)^2$

$$+ \quad \frac{(-2+d)(-3d^4p^4\xi+96320m^4\xi^2-115104dm^4\xi^2)}{1920(-5+d)(-3+d)m^4p^2\xi}($$ $)^2$

$$+ \quad \frac{(-2+d)(+48768d^2m^4\xi^2-8800d^3m^4\xi^2+576d^4m^4\xi^2)}{1920(-5+d)(-3+d)m^4p^2\xi}($$ $)^2$

$$+ \quad \frac{(-2+d)(-3128m^2p^2\xi^2+5832dm^2p^2\xi^2-3432d^2m^2p^2\xi^2)}{1920(-5+d)(-3+d)m^4p^2\xi}($$ 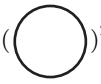 $)^2$

$$+ \quad \frac{(-2+d)(+792d^3m^2p^2\xi^2-64d^4m^2p^2\xi^2-60p^4\xi^2)}{1920(-5+d)(-3+d)m^4p^2\xi}($$ $)^2$

$$+ \quad \frac{(-2+d)(+107dp^4\xi^2-59d^2p^4\xi^2+13d^3p^4\xi^2-d^4p^4\xi^2)}{1920(-5+d)(-3+d)m^4p^2\xi}($$ $)^2$

$$+ \quad \frac{1680m^4-6840dm^4+6480d^2m^4-1320d^3m^4}{1920m^4}$$

$$+ \quad \frac{-240m^2p^2 + 640dm^2p^2 - 540d^2m^2p^2 + 140d^3m^2p^2}{1920m^4}$$

$$+ \quad \frac{56p^4 - 66dp^4 + 25d^2p^4 - 3d^3p^4 - 16080m^4\xi + 23640dm^4\xi}{1920m^4}$$

$$+ \quad \frac{-8400d^2m^4\xi + 840d^3m^4\xi + 400m^2p^2\xi - 720dm^2p^2\xi}{1920m^4}$$

$$+ \quad \frac{380d^2m^2p^2\xi - 60d^3m^2p^2\xi + 8p^4\xi - 14dp^4\xi}{1920m^4}$$

$$+ \quad \frac{7d^2p^4\xi - d^3p^4\xi - 6480m^4\xi^2 + 9720dm^4\xi^2}{1920m^4}$$

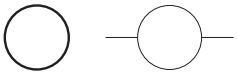

$$+ \quad \frac{-3600d^2m^4\xi^2 + 360d^3m^4\xi^2 - 2160m^4\xi^3}{1920m^4}$$

$$+ \quad \frac{3240dm^4\xi^3 - 1200d^2m^4\xi^3 + 120d^3m^4\xi^3}{1920m^4}$$

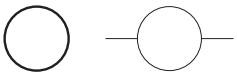

$$+ \quad \frac{16128m^4 - 37024dm^4 + 18272d^2m^4 - 2496d^3m^4}{960m^2p^2}$$

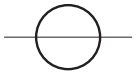

$$+ \quad \frac{-56m^2p^2 + 784dm^2p^2 - 1336d^2m^2p^2 + 384d^3m^2p^2}{960m^2p^2}$$

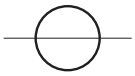

$$+ \quad \frac{168p^4 - 191dp^4 + 72d^2p^4 - 9d^3p^4 - 77056m^4\xi}{960m^2p^2}$$

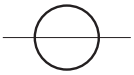

$$+ \quad \frac{67040dm^4\xi - 18912d^2m^4\xi + 1728d^3m^4\xi}{960m^2p^2}$$

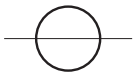

$$+ \quad \frac{-968m^2p^2\xi - 1312dm^2p^2\xi + 1112d^2m^2p^2\xi}{960m^2p^2}$$

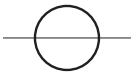

$$+ \quad \frac{-192d^3m^2p^2\xi + 24p^4\xi - 41dp^4\xi + 20d^2p^4\xi - 3d^3p^4\xi}{960m^2p^2}$$

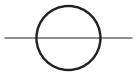

$$+ \quad \frac{(4m^2 + p^2)(-2016m^4 + 3872dm^4 - 832d^2m^4)}{960m^2p^2}$$

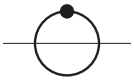

$$+ \quad \frac{(4m^2+p^2)(64m^2p^2-208dm^2p^2+128d^2m^2p^2)}{960m^2p^2}$$ 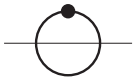

$$+ \quad \frac{(4m^2+p^2)(-28p^4+19dp^4-3d^2p^4+9632m^4\xi)}{960m^2p^2}$$ 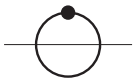

$$+ \quad \frac{(4m^2+p^2)(-4768dm^4\xi+576d^2m^4\xi-208m^2p^2\xi)}{960m^2p^2}$$ 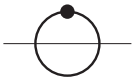

$$+ \quad \frac{(4m^2+p^2)(272dm^2p^2\xi-64d^2m^2p^2\xi)}{960m^2p^2}$$ 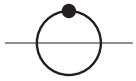

$$+ \quad \frac{(4m^2+p^2)(-4p^4\xi+5dp^4\xi-d^2p^4\xi)}{960m^2p^2}$$ 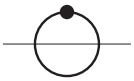

(51)

$F5_2 =$

$$- \quad \frac{416m^2-576dm^2+264d^2m^2-40d^3m^2}{48(-3+d)m^2p^2}($$ $$)^2$$

$$- \quad \frac{+48p^2-53dp^2+18d^2p^2-d^3p^2-608m^2\xi}{48(-3+d)m^2p^2}($$ $$)^2$$

$$- \quad \frac{768dm^2\xi-312d^2m^2\xi+40d^3m^2\xi-6p^2\xi}{48(-3+d)m^2p^2}($$ $$)^2$$

$$- \quad \frac{11dp^2\xi-6d^2p^2\xi+d^3p^2\xi}{48(-3+d)m^2p^2}($$ 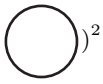 $$)^2$$

$$- \quad \frac{(-1+d)(4m^2+p^2)(-1+\xi)(-d-4\xi+d\xi)\Gamma[(-1+d)/2]}{32\Gamma(1/2+d/2)}$$ 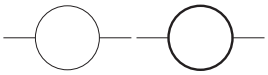

$$- \quad \frac{8(16m^2-8dm^2+3p^2-2dp^2-24m^2\xi)}{32}$$ 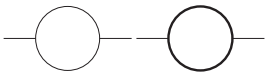

$$- \quad \frac{8(8dm^2\xi-6p^2\xi+2dp^2\xi)}{32}$$ 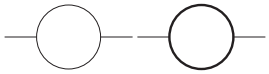

$$+ \quad 3(-1+d)m^2(-1+\xi)(-d-4\xi+d\xi)\Gamma[(-1+d)/2]$$

$$+\ \frac{192m^2-186dm^2+42d^2m^2+26p^2-15dp^2}{48m^2}$$

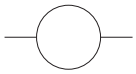

$$+\ \frac{d^2p^2-264m^2\xi+204dm^2\xi-36d^2m^2\xi}{48m^2}$$

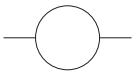

$$+\ \frac{-2p^2\xi+3dp^2\xi-d^2p^2\xi-24m^2\xi^2+30dm^2\xi^2}{48m^2}$$

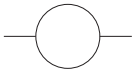

$$+\ \frac{-6d^2m^2\xi^2}{48m^2}$$

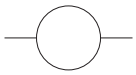

$$+\ \frac{-4m^2+4dm^2-3p^2+2dp^2}{8(-3+d)m^2}$$

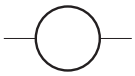

$$-\ \frac{p^2(8m^2+p^2)}{8}$$

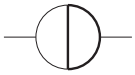

$$-\ \frac{1664m^2-2096dm^2+872d^2m^2-120d^3m^2}{24(-2+d)p^2}$$

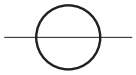

$$-\ \frac{288p^2-283dp^2+74d^2p^2-3d^3p^2-2432m^2\xi}{24(-2+d)p^2}$$

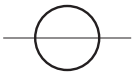

$$-\ \frac{2768dm^2\xi-1016d^2m^2\xi+120d^3m^2\xi-114p^2\xi}{24(-2+d)p^2}$$

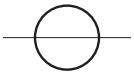

$$-\ \frac{121dp^2\xi-38d^2p^2\xi+3d^3p^2\xi}{24(-2+d)p^2}$$

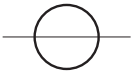

$$-\ \frac{2496m^4-3040dm^4+1216d^2m^4}{24(-3+d)(-2+d)p^2}$$

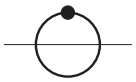

$$-\ \frac{-160d^3m^4+960m^2p^2-1068dm^2p^2+376d^2m^2p^2}{24(-3+d)(-2+d)p^2}$$

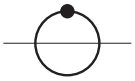

$$-\ \frac{-44d^3m^2p^2+96p^4-83dp^4+18d^2p^4-d^3p^4}{24(-3+d)(-2+d)p^2}$$

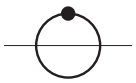

$$-\ \frac{-3648m^4\xi+4000dm^4\xi-1408d^2m^4\xi+160d^3m^4\xi}{24(-3+d)(-2+d)p^2}$$

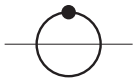

$$- \quad \frac{-936m^2p^2\xi + 1044dm^2p^2\xi - 376d^2m^2p^2\xi}{24(-3+d)(-2+d)p^2}$$ 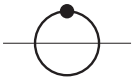

$$- \quad \frac{44d^3m^2p^2\xi - 6p^4\xi + 11dp^4\xi - 6d^2p^4\xi + d^3p^4\xi}{24(-3+d)(-2+d)p^2}$$ 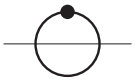

(52)

$F6_2 =$

$$\frac{(-2+d)(-1+d)d}{4(-3+d)m^2}($$ $$)^2$$

(53)

$F7_2 =$

$$\frac{3(-1+d+\xi)}{4}$$ 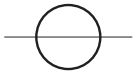

(54)

$F9_2 =$

$$\frac{(-2+d)(-1+d)(1-\xi+d\xi)}{8(-5+d)(-3+d)m^2\xi}($$ $$)^2$$

(55)

$F10_2 =$

$$- \quad \frac{(-1+d)(-14+43d-11d^2+134\xi-63d\xi)}{16}$$ 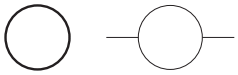

$$- \quad \frac{(-1+d)(7d^2\xi+54\xi^2-27d\xi^2)}{16}$$

$$- \quad \frac{(-1+d)(3d^2\xi^2+18\xi^3-9d\xi^3+d^2\xi^3)}{16}$$

(56)

**References**


1. K. Kajantie, M. Laine, K. Rummukainen and Y. Schroder, JHEP **0304**, 036 (2003) [arXiv:hep-ph/0304048].
2. A. D. Linde, Phys. Lett. B **96** (1980) 289.
3. P. H. Ginsparg, Nucl. Phys. B **170** (1980) 388.
4. T. Appelquist and R. D. Pisarski, Phys. Rev. D **23** (1981) 2305.
5. K. Kajantie, M. Laine, K. Rummukainen and M. E. Shaposhnikov, Nucl. Phys. B **458** (1996) 90 [arXiv:hep-ph/9508379].
   K. Kajantie, M. Laine, K. Rummukainen and M. E. Shaposhnikov, Phys. Rev. Lett. **77** (1996) 2887 [arXiv:hep-ph/9605288].
   K. Kajantie, M. Laine, K. Rummukainen and M. E. Shaposhnikov, Nucl. Phys. B **493** (1997) 413 [arXiv:hep-lat/9612006].
6. P. Giovannangeli, Phys. Lett. B **585** (2004) 144 [arXiv:hep-ph/0312307].
7. M. E. Shaposhnikov, [arXiv:hep-ph/9610247].
8. L. F. Abbott, Nucl. Phys. B **185** (1981) 189.
9. P. Giovannangeli, in preparation.
10. J. A. M. Vermaseren, [arXiv:math-ph/0010025].
11. R. Mertig and R. Scharf, Comput. Phys. Commun. **111**, 265 (1998) [arXiv:hep-ph/9801383].
12. O. V. Tarasov, Phys. Rev. D **54** (1996) 6479 [arXiv:hep-th/9606018].
13. O. V. Tarasov, Nucl. Phys. B **502** (1997) 455 [arXiv:hep-ph/9703319].
14. A. Hart and O. Philipsen, Nucl. Phys. B **572**, 243 (2000) [arXiv:hep-lat/9908041].
    A. Hart, M. Laine and O. Philipsen, Nucl. Phys. B **586**, 443 (2000) [arXiv:hep-ph/0004060].
15. G. Boyd, J. Engels, F. Karsch, E. Laermann, C. Legeland, M. Lutgemeier and B. Petersson, Nucl. Phys. B **469** (1996) 419 [arXiv:hep-lat/9602007].
16. M. Lutgemeier, Nucl. Phys. Proc. Suppl. **42** (1995) 523.
17. M. J. Teper, Phys. Rev. D **59**, 014512 (1999) [hep-lat/9804008].
18. B. Lucini and M. Teper, Phys. Rev. D **66** (2002) 097502 [arXiv:hep-lat/0206027]
19. F. Karsch, E. Laermann and M. Lutgemeier, Phys. Lett. B **346** (1995) 94 [hep-lat/9411020].
20. H. B. Meyer, JHEP **0401** (2004) 030 [hep-lat/0312034].
21. M.Lüscher, P.Weisz, JHEP**0109**(2001) 010 [hep-lat/0108014].
22. S. z. Huang and M. Lissia, Nucl. Phys. B **438** (1995) 54 [arXiv:hep-ph/9411293].
23. S. Necco, Nucl. Phys. B **683** (2004) 137 [arXiv:hep-lat/0309017].
    S. Necco and R. Sommer, Nucl. Phys. B **622** (2002) 328 [arXiv:hep-lat/0108008].
24. M. Laine and Y. Schroder, JHEP **0503** (2005) 067 [arXiv:hep-ph/0503061].
25. A. K. Rajantie, Nucl. Phys. B **480**, 729 (1996) [Erratum-ibid. B **513**, 761 (1998 NUPHA,B513,761-762.1998)] [arXiv:hep-ph/9606216].